EUROPEAN ORGANIZATION FOR NUCLEAR RESEARCH

CERN-PPE/91-27
13 February 1991

Measurement of Charge Asymmetry in Hadronic Z Decays

The ALEPH Collaboration

13 February 1991

Abstract

A significant charge asymmetry is observed in the hadronic Z decays collected with the ALEPH detector at LEP. The asymmetry expressed in terms of the difference in momentum weighted charges in the two event hemispheres is measured to be: $\langle Q_{Forward} \rangle - \langle Q_{Backward} \rangle = -0.0084 \pm 0.0015$ (stat.) ± 0.0004 (exp. sys.). In the framework of the Standard Model this can be interpreted as a measurement of the effective electroweak mixing angle, $\sin^2\theta_W(M_Z^2) = 0.2300 \pm 0.0034$ (stat.) ± 0.0010 (exp. sys.) ± 0.0038 (theor. sys.) or of the ratio of the vector to axial-vector coupling constants of the electron, $g_{Ve}/g_{Ae} = +0.073 \pm 0.024$.

(Submitted to Physics Letters B)

The ALEPH Collaboration

D. Decamp, B. Deschizeaux, C. Goy, J.-P. Lees, M.-N. Minard

Laboratoire de Physique des Particules (LAPP), IN^{2}P^3-CNRS, 74019 Annecy-le-Vieux Cedex, France

R. Alemany, J.M. Crespo, M. Delfino, E. Fernandez, V. Gaitan, Ll. Garrido, P. Mato, Ll.M. Mir, A. Pacheco

Laboratorio de Fisica de Altas Energias, Universidad Autonoma de Barcelona, 08193 Bellaterra (Barcelona), Spain[8]

M.G. Catanesi, D. Creanza, M. de Palma, A. Farilla, G. Iaselli,[1] G. Maggi, M. Maggi, S. Natali, S. Nuzzo, M. Quattromini, A. Ranieri, G. Raso, F. Romano, F. Ruggieri, G. Selvaggi, L. Silvestris, P. Tempesta, G. Zito

INFN Sezione di Bari e Dipartimento di Fisica dell' Università, 70126 Bari, Italy

Y. Gao, H. Hu,[21] D. Huang, X. Huang, J. Lin, J. Lou, C. Qiao,[21] T. Ruan,[21] Wang, Y. Xie, D. Xu, R. Xu, J. Zhang, W. Zhao

Institute of High-Energy Physics, Academia Sinica, Beijing, The People's Republic of China[9]

W.B. Atwood,[2] F. Bird, E. Blucher, G. Bonvicini, F. Bossi, D. Brown, T.H. Burnett,[2] H. Drevermann, F. Dydak, R.W. Forty, C. Grab, R. Hagelberg, S. Haywood, J. Hilgart, B. Jost, M. Kasemann, J. Knobloch, A. Lacourt, E. Lançon, I. Lehraus, T. Lohse, A. Marchioro, M. Martinez, J. May, S. Menary, A. Minten, A. Miotto, R. Miquel, H.-G. Moser, J. Nash, P. Palazzi, F. Ranjard, G. Redlinger, A. Roth, J. Rothberg,[2] H. Rotscheidt, R. St.Denis, D. Schlatter, M. Takashima, M. Talby,[4] W. Tejessy, H. Wachsmuth, S. Wasserbaech, S. Wheeler, W. Wiedenmann, W. Witzeling, J. Wotschack

European Laboratory for Particle Physics (CERN), 1211 Geneva 23, Switzerland

Z. Ajaltouni, M. Bardadin-Otwinowska, A. Falvard, R. El Fellous, P. Gay, J. Harvey, P. Henrard, J. Jousset, B. Michel, J-C. Montret, D. Pallin, P. Perret, J. Proriol, F. Prulhière, G. Stimpfl

Laboratoire de Physique Corpusculaire, Université Blaise Pascal, IN^{2}P^3-CNRS, Clermont-Ferrand, 63177 Aubière, France

J.D. Hansen, J.R. Hansen, P.H. Hansen, R. Møllerud, E.R. Nielsen, B.S. Nilsson

Niels Bohr Institute, 2100 Copenhagen, Denmark[10]

I. Efthymiopoulos, E. Simopoulou, A. Vayaki

Nuclear Research Center Demokritos (NRCD), Athens, Greece

J. Badier, A. Blondel, G. Bonneaud, J. Bourotte, F. Braems, J.C. Brient, G. Fouque, A. Gamess, R. Guirlet, S. Orteu, A. Rosowsky, A. Rougé, M. Rumpf, R. Tanaka, H. Videau

Laboratoire de Physique Nucléaire et des Hautes Energies, Ecole Polytechnique, IN^{2}P^3-CNRS, 91128 Palaiseau Cedex, France

D.J. Candlin, E. Veitch

Department of Physics, University of Edinburgh, Edinburgh EH9 3JZ, United Kingdom[11]

G. Parrini

Dipartimento di Fisica, Università di Firenze, INFN Sezione di Firenze, 50125 Firenze, Italy

M. Corden, C. Georgiopoulos, M. Ikeda, J. Lannutti, D. Levinthal,[16] M. Mermikides, L. Sawyer

Supercomputer Computations Research Institute and Dept. of Physics, Florida State University, Tallahassee, FL 32306, USA[13,14,15]

A. Antonelli, R. Baldini, G. Bencivenni, G. Bologna,[5] P. Campana, G. Capon, V. Chiarella, B. D'Ettorre-Piazzoli,[6] G. Felici, P. Laurelli, G. Mannocchi,[6] F. Massimo-Brancaccio, F. Murtas, G.P. Murtas, G. Nicoletti, L. Passalacqua, M. Pepe-Altarelli, P. Picchi,[5] P. Zografou

Laboratori Nazionali dell'INFN (LNF-INFN), 00044 Frascati, Italy

B. Altoon, O. Boyle, A.W. Halley, I. ten Have, J.L. Hearns, J.G. Lynch, W.T. Morton, C. Raine, J.M. Scarr, K. Smith, A.S. Thompson, R.M. Turnbull

Department of Physics and Astronomy, University of Glasgow, Glasgow G12 8QQ, United Kingdom[11]

B. Brandl, O. Braun, R. Geiges, C. Geweniger, P. Hanke, V. Hepp, E.E. Kluge, Y. Maumary, A. Putzer, B. Rensch, A. Stahl, K. Tittel, M. Wunsch

Institut für Hochenergiephysik, Universität Heidelberg, 6900 Heidelberg, Fed. Rep. of Germany[17]

A.T. Belk, R. Beuselinck, D.M. Binnie, W. Cameron, M. Cattaneo, P.J. Dornan,[1] S. Dugeay, A.M. Greene, J.F. Hassard, N.M. Lieske, S.J. Patton, D.G. Payne, M.J. Phillips, J.K. Sedgbeer, G. Taylor, I.R. Tomalin, A.G. Wright

Department of Physics, Imperial College, London SW7 2BZ, United Kingdom[11]

P. Girtler, D. Kuhn, G. Rudolph

Institut für Experimentalphysik, Universität Innsbruck, 6020 Innsbruck, Austria[19]

C.K. Bowdery,[1] T.J. Brodbeck, A.J. Finch, F. Foster, G. Hughes, N.R. Keemer, M. Nuttall, A. Patel, B.S. Rowlingson, T. Sloan, S.W. Snow, E.P. Whelan

Department of Physics, University of Lancaster, Lancaster LA1 4YB, United Kingdom[11]

T. Barczewski, L.A.T. Bauerdick, K. Kleinknecht, B. Renk, S. Roehn, H.-G. Sander, M. Schmelling, H. Schmidt, F. Steeg

Institut für Physik, Universität Mainz, 6500 Mainz, Fed. Rep. of Germany[17]

J-P. Albanese, J-J. Aubert, C. Benchouk, V. Bernard, A. Bonissent, D. Courvoisier, F. Etienne, S. Papalexiou, P. Payre, B. Pietrzyk, Z. Qian

Centre de Physique des Particules, Faculté des Sciences de Luminy, IN^{2}P^3-CNRS, 13288 Marseille, France

H. Becker, W. Blum, P. Cattaneo, G. Cowan, B. Dehning, H. Dietl, M. Fernandez-Bosman, T. Hansl-Kozanecka,[22] A. Jahn, W. Kozanecki,[2,23] E. Lange, J. Lauber, G. Lütjens, G. Lutz, W. Männer, Y. Pan, R. Richter, J. Schröder, A.S. Schwarz, R. Settles, U. Stierlin, J. Thomas, G. Wolf

Max-Planck-Institut für Physik und Astrophysik, Werner-Heisenberg-Institut für Physik, 8000 München, Fed. Rep. of Germany[17]

V. Bertin, J. Boucrot, O. Callot,[1] X. Chen, A. Cordier, M. Davier, G. Ganis, J.-F. Grivaz, Ph. Heusse, P. Janot, D.W. Kim,[20] F. Le Diberder, J. Lefrançois,[1] A.-M. Lutz, J.-J. Veillet, I. Videau, Z. Zhang, F. Zomer

Laboratoire de l'Accélérateur Linéaire, Université de Paris-Sud, IN^{2}P^3-CNRS, 91405 Orsay Cedex, France

S.R. Amendolia, G. Bagliesi, G. Batignani, L. Bosisio, U. Bottigli, C. Bradaschia, M. Carpinelli, M.A. Ciocci, R. Dell'Orso, I. Ferrante, F. Fidecaro, L. Foà, E. Focardi, F. Forti, A. Giassi, M.A. Giorgi, F. Ligabue, A. Lusiani, E.B. Mannelli, P.S. Marrocchesi, A. Messineo, L. Moneta, F. Palla, G. Sanguinetti, J. Steinberger, R. Tenchini, G. Tonelli, G. Triggiani, C. Vannini, A. Venturi, P.G. Verdini, J. Walsh

Dipartimento di Fisica dell'Università, INFN Sezione di Pisa, e Scuola Normale Superiore, 56010 Pisa, Italy

J.M. Carter, M.G. Green, P.V. March, T. Medcalf, I.S. Quazi, M.R. Saich, J.A. Strong, R.M. Thomas, L.R. West, T. Wildish

Department of Physics, Royal Holloway & Bedford New College, University of London, Surrey TW20 OEX, United Kingdom[11]

D.R. Botterill, R.W. Clifft, T.R. Edgecock, M. Edwards, S.M. Fisher, T.J. Jones, P.R. Norton, D.P. Salmon, J.C. Thompson

Particle Physics Dept., Rutherford Appleton Laboratory, Chilton, Didcot, OXON OX11 OQX, United Kingdom[11]

B. Bloch-Devaux, P. Colas, C. Klopfenstein, E. Locci, S. Loucatos, E. Monnier, P. Perez, J.A. Perlas, F. Perrier, J. Rander, J.-F. Renardy, A. Roussarie, J.-P. Schuller, J. Schwindling, B. Vallage

Département de Physique des Particules Elémentaires, CEN-Saclay, 91191 Gif-sur-Yvette Cedex, France[18]

J.G. Ashman, C.N. Booth, C. Buttar, R. Carney, S. Cartwright, F. Combley, M. Dinsdale, M. Dogru, F. Hatfield, J. Martin, D. Parker, P. Reeves, L.F. Thompson

Department of Physics, University of Sheffield, Sheffield S3 7RH, United Kingdom[11]

S. Brandt, H. Burkhardt, C. Grupen, H. Meinhard, L. Mirabito, E. Neugebauer, U. Schäfer, H. Seywerd

Fachbereich Physik, Universität Siegen, 5900 Siegen, Fed. Rep. of Germany[17]

G. Apollinari, G. Giannini, B. Gobbo, F. Liello, L. Rolandi, U. Stiegler

Dipartimento di Fisica, Università di Trieste e INFN Sezione di Trieste, 34127 Trieste, Italy

L. Bellantoni, J.F. Boudreau, D. Cinabro, J.S. Conway, D.F. Cowen,[24] A.J. DeWeerd, Z. Feng, D.P.S. Ferguson, Y.S. Gao, J. Grahl, J.L. Harton, J.E. Jacobsen, R.C. Jared,[7] R.P. Johnson, B.W. LeClaire, Y.B. Pan, J.R. Pater, Y. Saadi, V. Sharma, A.M. Walsh, J.A. Wear, F.V. Weber, M.H. Whitney, Sau Lan Wu, Z.L. Zhou, G. Zobernig

Department of Physics, University of Wisconsin, Madison, WI 53706, USA[12]

[1] Now at CERN.
[2] Permanent adddress: SLAC, Stanford, CA 94309, USA.
[3] Permanent address: University of Washington, Seattle, WA 98195, USA.
[4] Also Centre de Physique des Particules, Faculté des Sciences, Marseille, France
[5] Also Istituto di Fisica Generale, Università di Torino, Torino, Italy.
[6] Also Istituto di Cosmo-Geofisica del C.N.R., Torino, Italy.
[7] Permanent address: LBL, Berkeley, CA 94720, USA.
[8] Supported by CAICYT, Spain.
[9] Supported by the National Science Foundation of China.
[10] Supported by the Danish Natural Science Research Council.
[11] Supported by the UK Science and Engineering Research Council.
[12] Supported by the US Department of Energy, contract DE-AC02-76ER00881.
[13] Supported by the US Department of Energy, contract DE-FG05-87ER40319.
[14] Supported by the NSF, contract PHY-8451274.
[15] Supported by the US Department of Energy, contract DE-FC0S-85ER250000.
[16] Supported by SLOAN fellowship, contract BR 2703.
[17] Supported by the Bundesministerium für Forschung und Technologie, Fed. Rep. of Germany.
[18] Supported by the Institut de Recherche Fondamentale du C.E.A..
[19] Supported by Fonds zur Förderung der wissenschaftlichen Forschung, Austria.
[20] Supported by the Korean Science and Engineering Foundation and Ministry of Education.
[21] Supported by the World Laboratory.
[22] On leave of absence from MIT, Cambridge, MA 02139, USA.
[23] Supported by Alexander von Humboldt Fellowship, Germany.
[24] Now at California Institute of Technology, Pasadena, California, USA.

1 Introduction

A measurement of the charge asymmetry in an inclusive sample of hadronic events is used to study the forward-backward asymmetry (A_{FB}) in $Z \to q\bar{q}$ decays. At parton level A^f_{FB} for a single quark flavour f is defined as:

$$A^f_{FB} \equiv \frac{\sigma^f_F - \sigma^f_B}{\sigma^f_F + \sigma^f_B}. \tag{1}$$

This asymmetry causes the average charges produced in the forward and backward hemispheres, $\langle Q^f_F \rangle$ and $\langle Q^f_B \rangle$, to be different from zero: $\langle Q^f_F \rangle = q^f A^f_{FB}$, $\langle Q^f_B \rangle = -q^f A^f_{FB}$, where q^f is the quark charge. The charge flow, $Q_{FB} \equiv Q_F - Q_B$, the difference between the charges measured in the forward and backward hemispheres, has an average value for a single quark flavour f:

$$\langle Q^f_{FB} \rangle = 2q^f A^f_{FB}. \tag{2}$$

Near the Z pole the forward-backward, or charge, asymmetry arises from the difference between the left-handed and right-handed couplings of the Z both to the initial state leptons and the final state quarks. If one neglects the small QED effects, the asymmetry for massless quarks of flavour f at the Z pole can be written as:

$$A^f_{FB} = \frac{3}{4}\,\mathcal{A}_e\,\mathcal{A}_f\,; \quad \mathcal{A}_e = \frac{(g_{Le})^2 - (g_{Re})^2}{(g_{Le})^2 + (g_{Re})^2} = \frac{2\,g_{Ve}\,g_{Ae}}{(g_{Ve})^2 + (g_{Ae})^2}, \tag{3}$$

where $\mathcal{A}_e$ is the left-right asymmetry in the neutral current couplings of the electrons. The same formula holds for $\mathcal{A}_f$. The quantity $\mathcal{A}_e$ is small but very sensitive to $\sin^2\theta_W(M_Z^2)$. In relative terms, $\mathcal{A}_e$ is not well known experimentally [1] [2]. On the other hand, $\mathcal{A}_f$ is large and insensitive to $\sin^2\theta_W(M_Z^2)$. Furthermore, quark couplings have been measured in neutrino scattering experiments [1]. Consequently, a precise measurement of the quark asymmetry provides new information mostly on the electron couplings (in particular on the relative signs of g_{Ve} and g_{Ae}), and hence on the Standard Model parameter $\sin^2\theta_W(M_Z^2)$.

2 Method

As quarks are not observed directly, their charges have to be inferred from the resulting hadronic final states. Various e^+e^- experiments [3][4][5][6][7] have achieved this by using a weighted charge method originally proposed by Field and Feynman [8]. This method is based on the premise that there is a high probability that the original quark is contained in one of the leading hadrons. A correlation between the weighted charge of the hadrons and the parton charge has already been observed in neutrino and muon scattering experiments [9][10] where the current jet mainly originates from a single flavour.

Longitudinal momentum weighting with respect to the thrust axis of the event is used here. Other collaborations have weighted by pseudorapidity, longitudinal momentum of the particle with respect to the jet, or both. Alternative weighting schemes were found to yield similar charge finding efficiencies.

The conventions for geometry are shown in Fig. 1a. The thrust axis $\vec{e}_T$ is oriented so that it points in the forward direction (defined by the e^- beam). The event is separated in two hemispheres by a plane perpendicular to the thrust axis. The charge in the forward hemisphere is reconstructed as:

$$Q_F \equiv \frac{\sum^{\vec{p}_i.\vec{e}_T>0} |\vec{p}_i.\vec{e}_T|^\kappa \, q_i}{\sum^{\vec{p}_i.\vec{e}_T>0} |\vec{p}_i.\vec{e}_T|^\kappa}, \tag{4}$$

where q_i is the charge of particle i and κ is a weighting parameter. Similarly, in the backward hemisphere the charge Q_B is reconstructed using all particles with $\vec{p}_i.\vec{e}_T < 0$. Two quantities are formed from these charges: the charge flow $Q_{FB} = Q_F - Q_B$, and the total event charge $Q = Q_F + Q_B$.

As an example, Fig. 1b shows the Q_{FB} distributions for $Z \to u\bar{u}$ events as reconstructed from Monte Carlo simulation[1] of the hadronic final state where the u or $\bar{u}$ quark goes into the forward hemisphere. The difference between the means of the distributions demonstrates that the analysis at hadron level distinguishes between a u or a $\bar{u}$ quark going into the forward hemisphere. Similar distributions are obtained for other quark flavours. The charge separation $\delta^f \equiv \langle Q_{FB}^{f,forward} \rangle$ is obtained from the average value of Q_{FB} for events with a quark f going in the forward direction. At parton level $\delta^f = 2\,q^f$. At hadron level the average Q_{FB} of a *specific* quark flavour going in the forward direction is smaller than $2\,q^f$ (see Table 1)[2].

The average Q_{FB} in the inclusive hadronic event sample is a sum over the different quark flavours of their forward-backward asymmetry, weighted by the charge separations and the relative production rates:

$$\langle Q_{FB} \rangle = \sum_{f=1}^{5} \delta^f A_{FB}^f \frac{\Gamma_f}{\Gamma_{had}}, \tag{5}$$

where Γ_f is the Z partial width into quark f and Γ_{had} is the total hadronic width. Near the Z pole this can be written as:

$$\langle Q_{FB} \rangle \approx \frac{\cos\theta_{max}}{1 + \frac{1}{3}\cos^2\theta_{max}} \mathcal{A}_e \sum_{f=1}^{5} \delta^f \mathcal{A}_f \frac{\Gamma_f}{\Gamma_{had}} = C_{acc} \mathcal{A}_e \frac{2 \sum_f \delta^f g_{Af} g_{Vf}}{\sum_f (g_{Af})^2 + (g_{Vf})^2} = C \mathcal{A}_e \mathcal{F}, \tag{6}$$

[1]The partons are generated using the DYMU event generator [11] and are subsequently fragmented using the JETSET string fragmentation [12]. For the particle decays detailed heavy flavour decay tables are used.

[2]The value of δ^f for a c quark can be understood qualitatively. δ^f is smaller for a c than a u quark because the softness of the decay pion from a charged D^* results in a relatively low value of weighted charge.

quark flavour f	δ^f parton level	δ^f hadronic final state ($\kappa = 1$)
u	1.33	0.42
d	–0.67	–0.21
s	–0.67	–0.29
c	1.33	0.17
b	–0.67	–0.22

Table 1: The charge separation δ^f for different quark flavours as expected at parton level and in the hadronic final state.

where $\cos\theta_{max}$ defines the experimental polar angle acceptance, $\mathcal{F} \equiv \sum_f \delta^f g_{Af} g_{Vf}$, and C absorbs the remaining factors. Eq. 6 shows that $\langle Q_{FB} \rangle$ is proportional to $\mathcal{A}_e$ (which contains the main dependence on $\sin^2\theta_W(M_Z^2)$), multiplied by a factor $\mathcal{F}$. For $\sin^2\theta_W(M_Z^2) = 0.23$, the value of the product $g_{Af} g_{Vf}$ is smaller for u type quarks (0.38) than for d type quarks (0.69), but the charge separations are larger for u type quarks than for d type quarks and have opposite sign. This leads to some degree of cancellation and hence a smaller sensitivity of $\langle Q_{FB} \rangle$ to $\sin^2\theta_W(M_Z^2)$ than one would obtain for a single flavour. Near the Z pole the d type quarks will dominate $\langle Q_{FB} \rangle$ in spite of smaller δ^f because of the larger asymmetry, larger production cross section, and absence of top quark production. The factor $\mathcal{F}$ will be linearly dependent on the exact values of the charge separations δ^f, which have to be obtained from Monte Carlo simulations.

An experimental constraint on the various δ^f values is provided by analysis of the width of the distributions of Q_{FB} and Q. In the hadronic event sample these distributions consist of a superposition of the individual quark and antiquark distributions, centred around $\pm\delta^f$ respectively for Q_{FB} and around 0 in each case for Q. The total Q_{FB} distribution will thus be broadened with respect to the total Q distribution by an amount which can be interpreted as an effective charge separation $\bar{\delta}$:

$$\bar{\delta} \equiv \sqrt{\sigma^2_{Q_{FB}} - \sigma^2_Q} \approx \sqrt{\sum_{f=1}^{5} (\delta^f)^2 \frac{\Gamma_f}{\Gamma_{had}}}. \qquad (7)$$

The approximate validity of this equation makes use of the equalities: $\sigma^f_Q = \sigma^{\bar{f}}_Q$, $\sigma^f_{Q_{FB}} = \sigma^{\bar{f}}_{Q_{FB}}$, and $\delta^f = -\delta^{\bar{f}}$, as well as the near independence of Q_F and Q_B event by event. The quantity $\bar{\delta}$ is experimentally measurable and directly comparable with a Monte Carlo simulation. As the Q_{FB} and Q distributions are to a good approximation gaussian, their widths are statistically independent of their mean values. Therefore this test is independent of electroweak parameters but sensitive to fragmentation and detector simulation. Moreover, $\bar{\delta}$ is an indicator for the discrimination power of this

method of analysis: a typical value of $\bar{\delta}$ is 0.29, and of $\sigma_{Q_{FB}}$ is 0.61 ($\kappa = 1$).

The parameter κ can be chosen arbitrarily to optimize the sensitivity of the measurement. In previous experiments [3][4][5], κ was fixed by optimising the fraction of events that have oppositely signed weighted charge in the two event hemispheres. This opposite sign fraction is observed to decrease monotonically in the present analysis. The value chosen here is $\kappa = 1$. This optimizes the accuracy of the determination of $\sin^2\theta_W(M_Z^2)$ or g_{Ve}/g_{Ae} based on $\langle Q_{FB} \rangle$. Eq. 6 shows that the expected asymmetry is carried by the factor $\mathcal{F}$; therefore, one can obtain the best sensitivity for $\sin^2\theta_W(M_Z^2)$ with respect to $\langle Q_{FB} \rangle$ by optimizing $\mathcal{S} \equiv \mathcal{F}/\sigma_{Q_{FB}}$. This sensitivity $\mathcal{S}$ shown in Fig. 2 is found to have a clear extremum around $\kappa = 1$. This point of maximum statistical sensitivity was found to have the smallest error once the systematic errors were included. It was verified that repeating the analysis for various κ values from 0.2 to ∞ gives different but statistically consistent results.

3 The ALEPH Detector

A detailed description of the ALEPH detector is given in ref. [13].

The measurement of the charge asymmetry relies heavily on the excellent tracking information from the ALEPH Inner Tracking Chamber (ITC) and from the Time Projection Chamber (TPC). The eight coaxial drift chamber layers of the ITC provide coordinates in r-ϕ space in the region $|\cos\theta| < 0.97$. The TPC extends radially to 180 cm from the interaction point and provides up to 21 space points.

In the 1.5 T magnetic field of the ALEPH superconducting solenoid the ITC/TPC combined charged track momentum resolution for $|\cos\theta| < 0.8$. is $\Delta p_t = 0.0008 p_t^2$ (p_t in GeV/c). The probability of charge misidentification is estimated to be well under 0.01% of all tracks in hadronic events.

4 Event Selection

During the 1989 and 1990 data taking, ALEPH has accumulated 8.66 ± 0.18 pb^{-1}.

For this analysis only charged tracks are used. The following track selection is applied:

1. the distance of closest approach of the track to the vertex in the x-y plane (d_0) must be smaller than 2.0 cm;

2. the closest approach in the z-direction (z_0) must be less than 10.0 cm;

3. the track must consist of at least four TPC space points;

4. $|\cos\theta_{track}| < 0.95$;

5. the track must carry a momentum transverse to the incident beam direction larger than 200 MeV/c.

Hadronic events are required to contain five or more tracks which pass selection criteria 1-4. A total charged energy in excess of 0.1 $\sqrt{s}$ is required in order to reduce the background from photon events. The trigger efficiency for these events is measured to be 99.96±0.02% [14]. The analysis is restricted to a region of good resolution and acceptance by applying a cut on the thrust axis angle θ_T, $|\cos\theta_T| \leq 0.9$. Using these selection criteria a hadronic event sample of 175,110 events is obtained. The values of Q_F and Q_B are calculated using tracks that pass criteria 1-5. In ref. [14] it has been shown that the event shape variables such as the $\cos\theta_T$ distribution are correctly described by the Monte Carlo simulations. Since the two photon background in the hadronic sample is less than 3.0×10^{-3} and does not effect $\langle Q_{FB} \rangle$ by more than 3.0×10^{-3} of its value, it is neglected in this analysis.

5 Experimental Results

κ	$\langle Q_{FB} \rangle$	$\langle Q \rangle$	$\sigma_{Q_{FB}^{data}}$	$\sigma_{Q_{FB}^{MC}}$	$\bar{\delta}^{data}/\bar{\delta}^{MC}$
0.5	-0.0045 ± 0.0010	0.0022 ± 0.0008	0.410 ± 0.001	0.405 ± 0.001	1.013 ± 0.013
1.0	-0.0084 ± 0.0015	0.0014 ± 0.0013	0.608 ± 0.001	0.608 ± 0.001	0.992 ± 0.018
2.0	-0.0137 ± 0.0022	0.0009 ± 0.0020	0.907 ± 0.002	0.908 ± 0.002	0.975 ± 0.024
∞	-0.0188 ± 0.0035	0.0027 ± 0.0033	1.446 ± 0.004	1.450 ± 0.003	0.940 ± 0.048

Table 2: Observables in the charge asymmetry analysis as a function of κ.

Table 2 shows the values of the important observables in this analysis for various choices of the weighting parameter κ. As κ increases the low momentum tracks contribute less to the reconstructed charge. At $\kappa = \infty$ the reconstructed charge is based only on the leading track in the event hemisphere.

Over the whole κ range a significant charge asymmetry $\langle Q_{FB} \rangle$ is observed. The total average event charge $\langle Q \rangle$ is compatible with zero except for $\kappa = 0.5$ where low momentum tracks contribute significantly to the reconstructed charge. The comparison between Monte Carlo and data at low κ is sensitive to the accuracy of the modelling of track finding efficiency for low momentum tracks and of absorption or creation of low momentum tracks, e.g. in wall interactions. However, as these processes are forward-backward symmetric, $\langle Q_{FB}^f \rangle$ itself remains unchanged.

In Fig. 3a (3b) the Q_{FB} (Q) distribution observed in data is compared to the Monte Carlo prediction at $\kappa = 1$. The Monte Carlo gives an excellent description of the data.

Figure 4 shows $\langle Q_{FB} \rangle$ as a function of $\cos\theta_T$ for $\kappa = 1$. The figure clearly demonstrates that there is a significant charge asymmetry, which is concentrated in the high $\cos\theta_T$ bins.

Sources of experimental systematic errors on $\langle Q_{FB} \rangle$ may be divided into two classes. The most problematic effects are those that are forward-backward and charge asymmetric as they can generate a false electroweak asymmetry. Other effects that are forward-backward or charge asymmetric only, result in a dilution of $\langle Q_{FB} \rangle$ and produce an uncertainty proportional to $\langle Q_{FB} \rangle$. Detector related systematic errors are discussed here for the specific case $\kappa = 1$ (see Section 6 for choice) for the following sources which can generate false asymmetries:

1. **Momentum imbalance in tracking due to momentum bias**
   A possible momentum imbalance has been corrected using ALEPH muon pair data. The average muon momentum was forced to match expectations for both signs in each of twelve $\cos\theta_T$ bins. This correction is applied to the sagitta, has a precision of typically 10 μm and does not exceed 40 μm, corresponding to less than 1% of the momentum. Applying this correction to hadronic events shifts $\langle Q_{FB} \rangle$ by $(4.2 \pm 2.0) \times 10^{-4}$.

2. **Track losses**
   Track losses due to track overlap, TPC cracks and secondary decays at the edge of the fiducial regions of the TPC are accounted for in the Monte Carlo and represents a loss of about 1%. This has been confirmed by a scan of 3600 tracks in the data. A study of two prong events revealed that additional losses due to detector effects not simulated in the Monte Carlo were at the level of $(1 \pm 1) \times 10^{-3}$. Examination of a possible charge asymmetry in Monte Carlo and data tracks that pass all selection criteria but are near the cut for one of the criteria, leads to the conclusion that any artificial asymmetry arising from lost or marginal tracks is less than 3.0×10^{-4}.

3. **Tracks with unphysically high momenta**
   In 0.30% of the hadronic events, a single track with an unphysically high momentum ($p > 50$ GeV/c) is found, mainly as a result of reconstruction ambiguities due to overlapping tracks. Positively and negatively charged tracks with these anomalously high momenta are produced symmetrically in the two halves of the detector, and therefore do not influence the charge asymmetry measurement. Moreover, this effect is correctly represented in the Monte Carlo. The systematic error due to these events has been obtained by studying the difference in $\langle Q_{FB} \rangle$ between the case where the events were included and the case

where they were excluded from the analysis. The resulting error on $\langle Q_{FB} \rangle$ is less than 0.6×10^{-4}.

4. **Loss or creation of secondary charged tracks in material between the vertex and the TPC**
   Interaction of particles in the material between the vertex and the TPC is potentially charge asymmetric due to charge dependent nuclear cross-sections. Both particle absorption and creation affect $\langle Q_F \rangle$ and $\langle Q_B \rangle$ equally and therefore have no influence on $\langle Q_{FB} \rangle$ but result in $\langle Q \rangle$ being non-zero. Particle absorption or creation can only cause an asymmetry if there is a difference between the amounts of material in the two hemispheres. Using photon conversions the material asymmetry A_{mat} is determined to be $-2.0 \pm 1.2\%$, while $\langle Q \rangle$ is measured to be 0.0014 ± 0.0013. Consequently the error on $\langle Q_{FB} \rangle$, estimated from $\langle Q \rangle \times A_{mat}$, is found to be less than 0.6×10^{-4}.

In addition the measurement of $\langle Q_{FB} \rangle$ is influenced by detector acceptance, resolution, etc. These detector effects are included in the detector simulation and are found to represent a 12% reduction in the expected value of $\langle Q_{FB} \rangle$. The accuracy with which these effects have been simulated can be expressed in terms of $\bar{\delta}^{data}/\bar{\delta}^{MC}$. As this ratio is found to be 0.992 ± 0.018 an additional systematic error of 1.5×10^{-4} is assigned to $\langle Q_{FB} \rangle$. An overview of the experimental systematic errors is given in Table 3.

To summarize, $\langle Q_{FB} \rangle$ is measured to be (for $\kappa = 1$):

$$\langle Q_{FB} \rangle = -0.0084 \pm 0.0015(\text{stat.}) \pm 0.0004(\text{exp.sys.}).$$

Source of systematic uncertainty	$\Delta \langle Q_{FB} \rangle$ (10^{-4})
Effects creating a false asymmetry:	
momentum imbalance	2.0
track losses	3.0
unphysically high momenta	0.6
presence of material	0.6
Dilution due to acceptance, resolution, etc.	1.5
Total experimental error	4.0

Table 3: Summary of the experimental systematic errors on $\langle Q_{FB} \rangle$.

6 Theoretical Uncertainties in the Charge Separations

The systematic uncertainty in the interpretation of $\langle Q_{FB} \rangle$ in terms of electroweak parameters (Eq. 6) stems mainly from the charge separation dependence on the fragmentation parameters in the Monte Carlo simulation. While the default values of these parameters yield $\bar{\delta}^{data}/\bar{\delta}^{MC} \simeq 1.0$, uncertainties in these parameters result in errors on the flavour dependent charge separations δ^f. The uncertainty can be expressed in terms of an error on $\mathcal{F}$ ($=\sum \delta^f g_{Af} g_{Vf}$) or of an error on the extracted values for $\sin^2\theta_W(M_Z^2)$ or g_{Ve}/g_{Ae}.

The systematic errors determined from variations of eleven fragmentation parameters in JETSET Version 6.3 are listed in Table 4. The ranges of variations of these parameters are either based on measurements [15] [16][17][18][19][20] or are given by theoretical constraints. A discussion of the choice of ranges is given in the Appendix.

The main error on $\mathcal{F}$ in JETSET stems from the uncertainty on the ratio s/u. The total error on $\mathcal{F}$ due to uncertainties in the fragmentation parameters of the JETSET string fragmentation is estimated to be 13.5%.

The model dependence of the flavour dependent charge separations has been investigated using the HERWIG Monte Carlo [21], which is based on cluster fragmentation. The value of $\mathcal{F}$ in HERWIG is found to be 15% larger than in JETSET 6.3. Since JETSET has shown its validity in reproducing charge flow in deep inelastic scattering, the value estimated by JETSET is kept as the central value. An additional systematic error of 15% is assigned to account for the difference with HERWIG.

Although some parameter variations may be incompatible with $\bar{\delta}^{data}/\bar{\delta}^{MC} \simeq 1.0$, this is not used to constrain the systematic error further because of possible correlations. Combining the uncertainty due to the JETSET parameters with that due to the choice of fragmentation model, the total systematic error in $\mathcal{F}$ is taken to be 20%.

7 Determination of the Electroweak Mixing Angle and the Electron Coupling Constants

The charge asymmetry $\langle Q_{FB} \rangle$ is measured over an eleven point energy scan around the Z mass covering the range $\sqrt{s}$ = 88.25 - 95.00 GeV. The theoretical predictions of $A_{FB}^f(s)$ for the different values of $\sin^2\theta_W(M_Z^2)$ have been calculated using EXPOSTAR [22], which includes exponentiated second order initial state radiation and electroweak corrections. The difference in event statistics at the various energies has been taken into account by weighting the contributions by the number of hadronic events recorded at each energy. This energy averaging is allowed as A_{FB} varies almost linearly with energy in the energy region studied. Taking the measurement of $\langle Q_{FB} \rangle$

parameter	range	$\frac{\Delta\mathcal{F}}{\mathcal{F}}$ (%)
Λ_{QCD}	0.26 - 0.40 GeV	4.4
M_{min}	1.0 - 2.0 GeV	2.2
b	0.85 - 0.93	2.8
σ	0.34-0.40	1.9
ε_c	0.002 - 0.071	3.7
ε_b	0.003 - 0.010	4.4
$[V/(V+PS)]_{u,d}$	0.3 -0.75	3.5
$[V/(V+PS)]_s$	0.5 -0.75	1.0
$[V/(V+PS)]_{c,b}$	0.65 -0.8	2.8
s/u	0.27 - 0.40	8.7
χ	0.11 - 0.16	4.2

Table 4: Variation in the predicted value of $\mathcal{F}$ for changes in the fragmentation parameters. The statistical error on the uncertainties is 1.2%.

integrated over all energies one finds:

$$\sin^2\theta_W(M_Z^2) = 0.2300 \pm 0.0034(\text{stat.}) \pm 0.0010(\text{exp.sys.}) \pm 0.0038(\text{theor.sys.}). \quad (8)$$

As a check, Fig. 5 shows $\langle Q_{FB} \rangle$ as a function of $\sqrt{s}$. The data have been combined into three bins, one below, one at, and one above the Z pole. The theoretical curves give an acceptable description of the energy dependence of $\langle Q_{FB} \rangle$ as observed in the data.

As discussed above, the observed charge asymmetry can be expressed in terms of the electron and the quark couplings. Therefore the measurement of $\langle Q_{FB} \rangle$ can be used directly to determine $\mathcal{A}_e$ or g_{Ve}/g_{Ae}. The u and d quark coupling constants have been extracted from neutrino-nucleon scattering measurements [1]:

$$(g_{Lu})^2 + (g_{Ld})^2 = 0.2996 \pm 0.0044, \quad (9)$$

$$(g_{Ru})^2 + (g_{Rd})^2 = 0.0298 \pm 0.0038, \quad (10)$$

$$\tan^{-1}\left(\frac{g_{Lu}}{g_{Ld}}\right) = 2.47 \pm 0.04, \quad (11)$$

$$\tan^{-1}\left(\frac{g_{Ru}}{g_{Rd}}\right) = 4.65 \pm 0.40. \quad (12)$$

Assuming $\mathcal{A}_u = \mathcal{A}_c$ and $\mathcal{A}_d = \mathcal{A}_s = \mathcal{A}_b$, and using the δ^f values from the present analysis, the above values of the quark coupling constants yield: $\mathcal{A}_u$ =0.64 $\pm$ 0.08, $\mathcal{A}_d$ = 0.96 $\pm$ 0.05, and $\sum \delta^f A_f \Gamma_f / \Gamma_{had}$ = -0.086 $\pm$ 0.024.

Combining the numbers above with the measurement of $\langle Q_{FB} \rangle$ yields:

$$\mathcal{A}_e = +0.145 \pm 0.048 \quad (13)$$

or

$$\frac{g_{Ve}}{g_{Ae}} = +0.073 \pm 0.024. \quad (14)$$

The value expected from the Standard Model is ~ 0.070 for $\sin^2\theta_w(M_Z^2) = 0.232$.

The measurement presented in this paper establishes that the *signs* of g_{Ae} and g_{Ve} are the same.

8 Conclusions

A significant charge asymmetry is observed in hadronic Z decays:

$$\langle Q_{FB} \rangle = -0.0084 \pm 0.0015(\text{stat.}) \pm 0.0004(\text{sys.}). \quad (15)$$

In the framework of the Standard Model the measurement of $\langle Q_{FB} \rangle$ is interpreted in terms of $\sin^2\theta_W(M_Z^2)$:

$$\sin^2\theta_W(M_Z^2) = 0.2300 \pm 0.0034(\text{stat.}) \pm 0.0010(\text{exp.sys.}) \pm 0.0038(\text{theor.sys.}). \quad (16)$$

The main systematic error is found to be due to uncertainty in the fragmentation process. $\langle Q_{FB} \rangle$ can also be used to extract the electron left-right asymmetry $\mathcal{A}_e$ or the ratio of the electron couplings g_{Ve}/g_{Ae}. Assuming quark universality one finds $g_{Ve}/g_{Ae} = +0.073 \pm 0.024$.

Acknowledgements

We wish to congratulate and thank our colleagues in the LEP division for operating the LEP storage ring with continuously improving performance. We thank also the engineers and technicians in all our institutions for their support in constructing ALEPH. Those of us from non-member countries thank CERN for its hospitality.

Appendix - Sensitivity of $\langle Q_{FB} \rangle$ to JETSET Fragmentation Parameters

The values of Λ_{QCD} given by the different e^+e^- experiments range from 0.26 [18] to 0.40 GeV [19][20].

Most experiments have determined the best value for the minimum mass in the parton shower evolution, M_{min}, to be 1.0 GeV. As the ALEPH data favour a value around 1.50 $\pm$ 0.12 GeV [15], M_{min} for this study has been varied from 1.0 up to 2.0 GeV.

For a and b in the light quark string fragmentation two sets of preferred values exist, $a \approx 0.5$, $b \approx 0.9$ [15][19][20] and $a \approx 0.18$, $b \approx 0.34$ [17][18]. The latter setting, in combination with the ALEPH tuning for the other fragmentation parameters, yields a charged particle multiplicity that is too high by one track per event. Since the error on the ALEPH measurement of multiplicity is $\pm$ 0.45 [15], only the former setting is studied. As a and b are strongly correlated it is sufficient to vary b between 0.85 and 0.93 while keeping a fixed at 0.5 [15].

The parameter, σ, describing the width of the transverse momentum distribution of physical particles produced in the fragmentation has been varied between 0.34 and 0.40 GeV/c. This almost covers the full range of measured values from the various experiments [15]-[20].

The variation of ε_c and ε_b is based on ALEPH heavy flavour studies [16].

The vector to vector plus pseudoscalar ratios, V/(V+PS), are poorly known. For this study the ratios have been varied around the JETSET default values. The maximum values are set by a theoretical constraint. For light quarks the maximum is 3/(1+3)=0.75, while for heavy quarks the ratio can go up to 0.8 due to mass effects. The lower limits were obtained by varying the default settings down by the amount they differ from the maximum (as vector particles are observed it is unphysical to reduce the vector to pseudoscalar ratio to zero). HRS [23] and JADE [24] parameterized the pseudoscalar to vector rate as $PS/V = (1/3)(m_v/m_p)^{0.55}$. This leads to V/(V+PS) values of 0.54 for (V=ρ^0, PS=π^0), 0.69 for (V=K^{0*}, PS=K^0), and 0.74 for (V=D^{0*}, PS=D^0). In each case the value obtained is contained in the range over which the respective vector to pseudoscalar ratios are varied here.

The review of measurements of the ratio s/u given in ref. [25] sets the range to 0.27-0.37. As all these measurements were carried out at lower energies the range of s/u has been extended up to 0.40 to allow for possible increased strangeness production at LEP energies.

The influence of B^0-$\bar{B}^0$ mixing has also been investigated. For the charge reconstruction, all charged fragments or decay products of the b quark are used. Due to the different time scales for mixing and fragmentation, the b quark will have fragmented to a neutral object, a $\bar{B}^0$, long before it mixes to a B^0. The only bias B^0-$\bar{B}^0$ mixing can give in this analysis comes from the difference between the contributions to the hemisphere charge of the B^0 decay products once they are momentum weighted. The

effect of B^0-$\bar{B}^0$ mixing has been studied by varying the mixing parameter χ between 0.11 and 0.16, which is the range presently set by the ALEPH data [16].

References

[1] U. Amaldi et al., Phys. Rev. D36 (1987) 1385.

[2] CHARM-II collab., D. Geiregat., et al., CERN-PPE/91-15 (1991).

[3] Amy collab., D. Stuart et al., Phys. Rev. Lett. 64 (1990) 983.

[4] JADE collab., T. Greenshaw et al., Z. Phys. C42 (1989) 1.

[5] Mac collab., W.W. Ash et al., Phys. Rev. Lett. 58 (1987) 1080.

[6] PLUTO collab., Ch. Berger et al., Nucl. Phys. B214 (1983) 189.

[7] TASSO collab., R. Brandelik et al., Phys. Lett. 100B (1981) 357.

[8] R.D. Field and R.P. Feynman, Nucl. Phys. B136 (1978) 1.

[9] J.P. Berge et al., Nucl. Phys. B184 (1981) 13.

[10] EMC collab., J.P. Albanese et al., Phys. Lett. 144B (1984) 302.

[11] J.E. Campagne, Ph.D. Thesis, Paris, report LPNHEP 89-02;
J.E. Campagne and R. Zitoun, Z. Phys. C 43 (1989) 469.

[12] M. Bengtsson and T. Sjöstrand, Phys Lett. B 185 (1987) 435.

[13] ALEPH collab., D. Decamp et al., Nucl. Instr. A294 (1990) 121.

[14] ALEPH collab., D. Decamp et al., Z. Phys. C48 (1990) 365.

[15] ALEPH collab., K. Smith, in Proceedings of the 25th Rochester Conference, Singapore, 1990.

[16] ALEPH collab., D. Decamp et al., Phys. Lett. B244 (1990) 551.
ALEPH collab., D. Decamp et al., CERN-PPE/90-194 (1990).

[17] OPAL collab., M.Z. Akrawy et al., Z. Phys. C47 (1990) 505.

[18] TASSO collab., W. Braunschweig et al., Z. Phys. C41 (1988) 359.

[19] Mark II collab., A. Petersen et al., Phys. Rev. D37 (1988) 1.

[20] Amy collab., Y.K. Li et al., Phys. Rev. D41 (1990) 2675.

[21] G. Marchesini and B. Webber, Nucl. Phys. B310 (1988) 461;
I.G. Knowles, Nucl. Phys. B310 (1988) 571.

[22] D.C. Kennedy et al., Nucl. Phys. B321 (1989) 83-107.

[23] HRS collab., M. Derrick et al., Phys. Rev. Lett. 54 (1985) 2568.

[24] JADE collab., W. Bartel et al., Phys. Lett. B145 (1985) 441.

[25] D.H. Saxon in "High Energy Electron-Positron Physics" by A. Ali and P. Söding, (1988), 539.

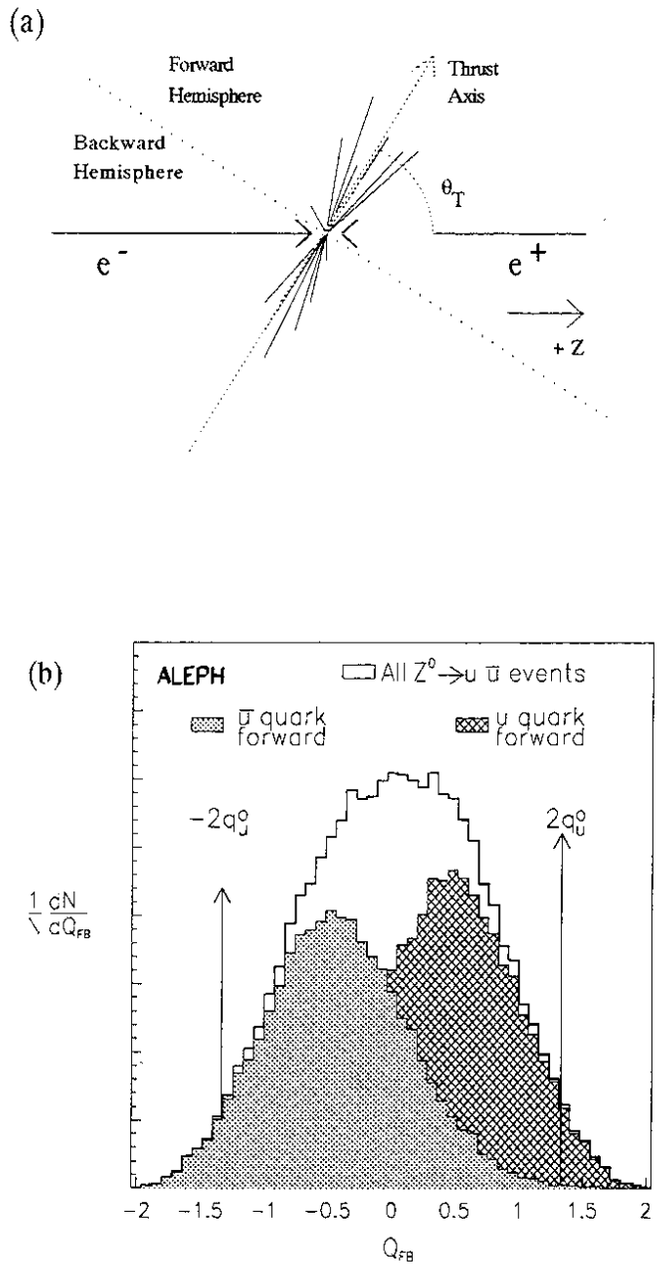

Figure 1: (a) Schematic of an $e^+e^- \to$ q $\bar{\text{q}}$ collision. Thrust axis is defined to be pointing in the electron ($+z$) direction. (b) Simulated distribution of $\frac{1}{N}\frac{dN}{dQ_{FB}}$ for three cases: i) the quark in the forward hemisphere is a u (solid); ii) the quark in the forward hemisphere is a $\bar{\text{u}}$ (hatched); iii) the quark in the forward hemisphere is either u or $\bar{\text{u}}$ (unfilled). Arrows at $\pm\frac{4}{3}$ indicate the Q_{FB} values expected if the quarks were directly observed.

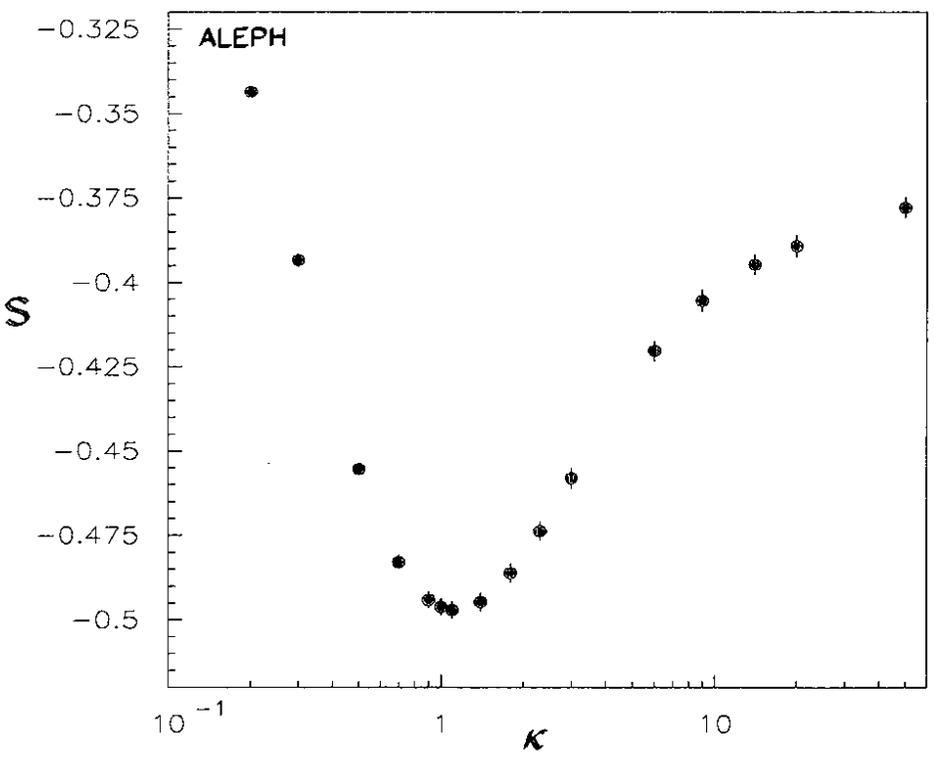

Figure 2: Monte Carlo calculations of the sensitivity $\mathcal{S} \equiv \mathcal{F}/\sigma_{Q_{FB}}$ as a function of κ.

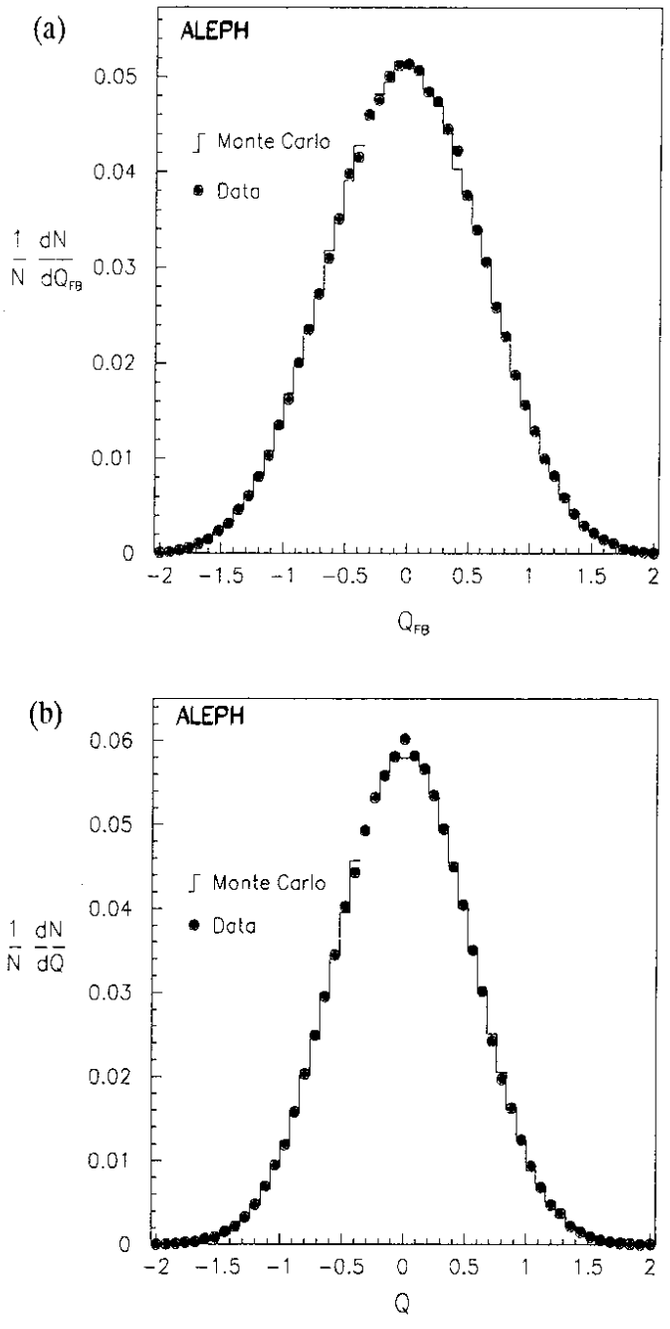

Figure 3: (a) Comparison of Q_{FB} distributions for data (black dots) and reconstructed Monte Carlo events (histogram). (b) Comparison of total event charge Q distributions for data (black dots) and reconstructed Monte Carlo events (histogram).

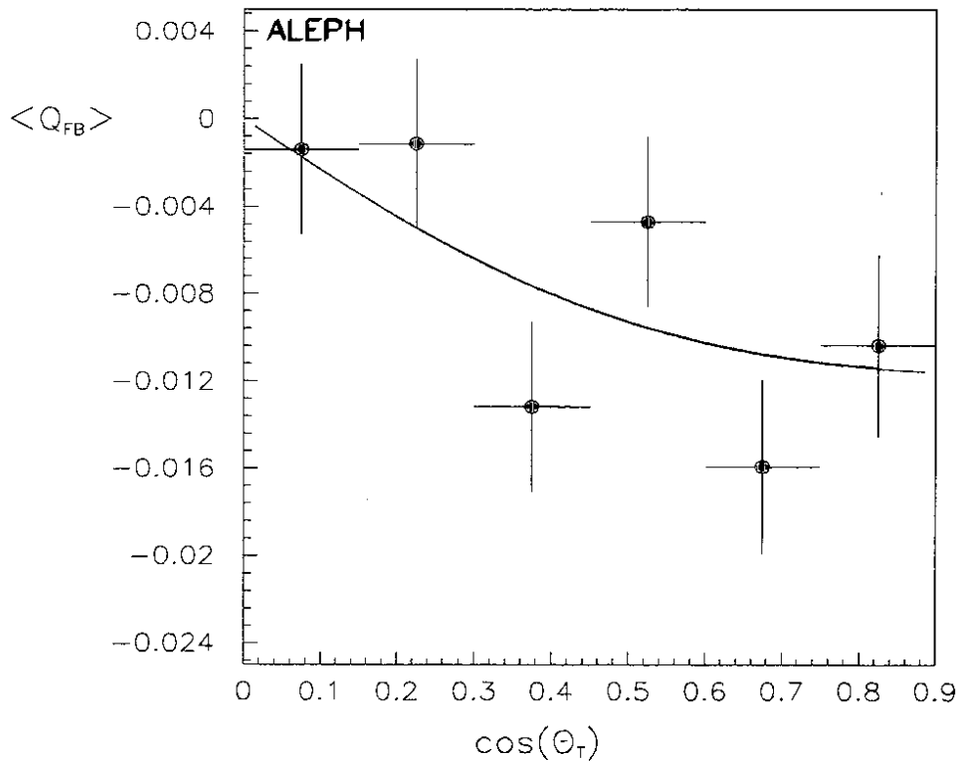

Figure 4: $\langle Q_{FB} \rangle$ as a function of $\cos\theta_T$. The fitted curve shows the prediction for $\sin^2\theta_W(M_Z^2) = 0.230$ (χ^2/D.O.F.=6.2/5).

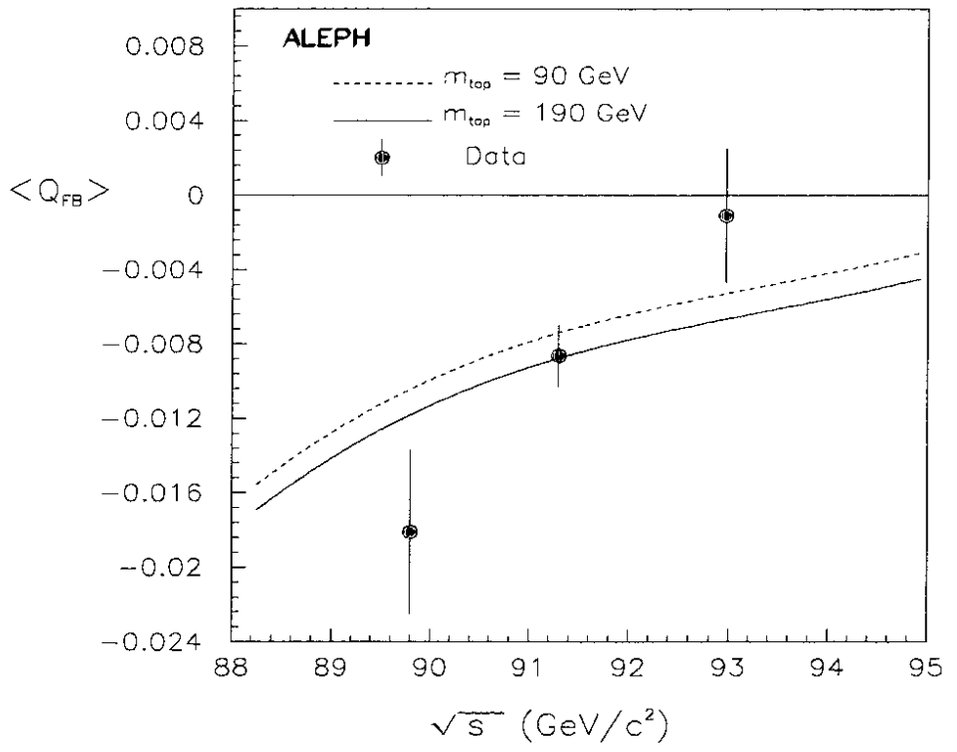

Figure 5: Predicted values of $\langle Q_{FB} \rangle$ for m_{top} = 190 GeV/c^2 (solid curve) and m_{top} = 90 GeV/c^2 (dashed curve), generated using the **EXPOSTAR** Monte Carlo [22]. In both cases m_{higgs} = 200 GeV/c^2 is assumed. Data points correspond to the measured $\langle Q_{FB} \rangle$ below, on, and above the Z pole.